[1]Lili Jin

[2]Jinsheng Chen

Traffic Accident Analysis and Prediction Model Based on Highway Pedestrian Prediction Using Deep Learning Model

Journal of Electrical Systems

Abstract: - Due to the high number of deaths, injuries, and fatalities as well as the enormous financial losses they cause every year, traffic accidents rank among the world's most serious worries. Road accidents can be caused by a variety of circumstances. It might be able to take action to lessen the severity and extent of the effects if these elements are better understood and forecast. In order to analyse the data, uncover hidden patterns, forecast the accident severity, and compile the information in an understandable manner, machine learning techniques are employed. In this research the novel deep learning model has been proposed for highway traffic accident analysis based on pedestrian detection in image analysis. here the highway traffic images has been collected and analysed for pedestrian detection using histogram residual Hopfield convolutional neural networks (HRHCNN) and feature selected using markov belief gradient discriminant analysis (MBGDA). the segmented selected features shows the detected pedestrian in highway traffic accident. In simulation results the various pedestrian dataset has been analysed in terms of AUC, F1 score, MCC, ATA, recall. The proposed technique achieved Average F-1 score was 82%, recall was 90%, AUC was 85%, ATA was 98%, and MCC was 96%.

Keywords: traffic accident analysis, pedestrian detection, deep learning model, Hopfield convolution, belief gradient

1. Introduction:

The number of pedestrian traffic crashes is still high due to world's population expansion as well as growing complexity of road conditions. Statistics on international crashes show that senior pedestrians are one of the most susceptible demographics on the road. Between 1990 and 2018, the number of pedestrian fatalities in the US grew by more than 3%. According to 2017 data, just 15.42% of Americans are over 65. In contrast, death rate from road pedestrian crashes among those over 65 is as high as 19.7%, representing an increase of 8.4 percentage points from 1985 data. With 281 and 271 deaths per 100,000 individuals, age groups with the highest total pedestrian fatality rates were 55–59 and 75–79 years old [1]. In contrast, statistics from the NHTSA's National Pedestrian Crash Report indicate a decrease in pedestrian fatalities from 1997 to 2006. It is also discovered that individuals over 64 had a significantly higher chance of dying in a collision than people in other age groups. Surprisingly, there were almost two pedestrian fatalities in car crashes for every 100,000 people in the country, and one pedestrian crash death for every 70 million kilometres travelled. This outcome is far lower than the senior population's death rate. This means that in pedestrian traffic crashes, older pedestrians still warrant special attention because they are a particularly vulnerable category [2]. Fewer research have been conducted on traffic crashes involving elderly pedestrians, though, because the total number of these incidents is rather low when compared to other age groups. Prediction studies, however, found that as the population ages, it is anticipated that there will be more than 83.7 million Americans over the age of 64 in 2050. The ageing population is driving up the need for increased road safety for older pedestrian groups, who are more likely to die in traffic accidents. To compare their surroundings and behaviour to those of other age groups, more investigation and study are needed [3]. Determining the significance of contributing elements to injury severity is made easier by machine learning approaches to accident data analysis from various scenarios. This makes it easier to choose relevant input data for development of predictive methods. Predictive methods are methods that use strongly correlated parameters as input features to forecast the degree of injuries sustained in accidents. The nonlinear link between injury severity and several accident-related factors is a significant difficulty for creating predictive models since injury severity is a complicated phenomena influenced by a wide range of contributing factors. Pedestrian detection technology finds widespread application in industries such as intelligent auxiliary driving, video surveillance, intelligent robots, and human behaviour analysis. It is also a research intersection, spanning multiple fields including artificial intelligence, pattern recognition, and target detection. However, due

[1] Guangzhou Vocational College of Technology &Business, Guangzhou, Guangdong Province, 511442 CHINA

Email address list :

Lili Jin : jinlili@gzkmu.edu.cn

Jinsheng Chen : Chenjs0429@163.cn

to the complicated background, variable pedestrian stance, and partial cover issue, this work presents several difficulties. There are numerous pedestrian detection techniques, but each has advantages and disadvantages of its own. The majority of current algorithms can only select between effectiveness and efficiency, and the same algorithm may produce different outcomes in various application contexts. Generally speaking, there are two types of pedestrian detection techniques: statistical learning and backdrop modelling. The latter is currently more widely used because it is based on defining high-level features with deep networks, whereas the former, like the Vibe method, is a pixel-level video backdrop modelling approach with specific limits in memory consumption and computing [4]. For instance, there are numerous intriguing deep learning-based detection and classification techniques. Therefore, the primary objective of this design is to create an effective, reliable, and useful pedestrian detector [5].

2. Background and related works:

Determining the significance of contributing elements to injury severity is made easier by machine learning approaches to accident data analysis from various scenarios. This makes it easier to choose relevant input data for development of predictive methods. Predictive methods are methods that use strongly correlated parameters as input features to forecast the degree of injuries sustained in accidents. The nonlinear link between injury severity and several accident-related factors is a significant difficulty for creating predictive models since injury severity is a complicated phenomena influenced by a wide range of contributing factors. Moreover, deep learning is being used more and more in accident analysis as a new analytics method. Long Short-Term Memory (LSTM) and Convolutional Neural Networks (CNN) are two popular deep learning methods [6]. Goal of the research governed by [7] was to develop a machine learning system for categorising different types of crashes involving pedestrians and bicycles from unstructured data, such as information from police reports. With an accuracy rate of up to 77% for training data and 72% for test data, the XGBoost model proved to be the most successful in detecting crash types among the data that the researchers gathered from two locations in Texas. The study [8] contrasted elements found in and outside of cities. The study revealed that the severity of accidents was influenced by several factors both inside and outside of urban areas. Within urban areas, the elements that affected accident severity were bicycles, junctions, young drivers, and collisions with objects. [9] examined the use of support vector machines (SVM), closest neighbour classification (NNC), Multinomial Logit (MNL), and RF analysis techniques to predict the severity of traffic incidents. According to the findings, NNC outperforms RF, SVM, and MNL in terms of overall prediction performance for more serious accidents. In order to predict traffic accidents, studies [10] examined a number of ML methods, including random forest, K-nearest neighbour, Bayesian network. The best model had a 38% false alert rate but could predict 61% of incidents. In order to train and test a classifier that predicts accidents with a training and testing accuracy of 55%, author [11] developed a CART (classification and regression trees) model. Poisson, negative binomial, and negative multinomial regression models were employed in Work [12] to forecast the frequency of accidents on multi-lane roadways. The author [13] examined current research on the forecasting of auto accidents. The authors discovered that while combining a variety of data sources, neural networks and deep learning techniques demonstrated great accuracy and precision. It's also important to note that data mining techniques are used in most road accident data analysis in an effort to pinpoint variables that affect an accident's severity. As per reference [14], data mining techniques like clustering algorithms, classification, and association rule mining, along with the identification of accident-prone regions, are highly beneficial in assessing the different pertinent elements of traffic accidents. Finding accident hotspots is another crucial factor and typically the initial stage of road safety studies. Inaccuracies in identification of hotspots could produce inferior outcomes. A comparison of common HotSpot IDentification (HSID) techniques has been done in work [15]. Among the techniques is the empirical Bayes approach (EB), which has outperformed the other HSID techniques and been shown to be the most consistent and dependable technique. Using the GPS coordinates of the accidents, the study by [16] applies a clustering technique (DBSCAN) to search for accident hotspots as an alternative to conventional HSID techniques. The DBSCAN algorithm makes it possible to identify hotspots, also known as clusters, that have a high accident density and shorter lengths. Low-density areas will also be eliminated by the algorithm.

3. Material and methods:

Figure 1 depicts a flowchart that describes the overall process used in this work to assess the seriousness of the vehicle-pedestrian collision. This study's input layer gathers numerical data on collisions between cars and

pedestrians. The hidden layer then applies a number of mathematical operations on the incoming input in order to identify data patterns. The weighted total of the inputs and a transfer function are used to calculate the bias after each input node has been assigned a weight. The prediction results are also contrasted with a predetermined threshold that is used to categorise the severity of vehicle-pedestrian collisions based on the activation function.

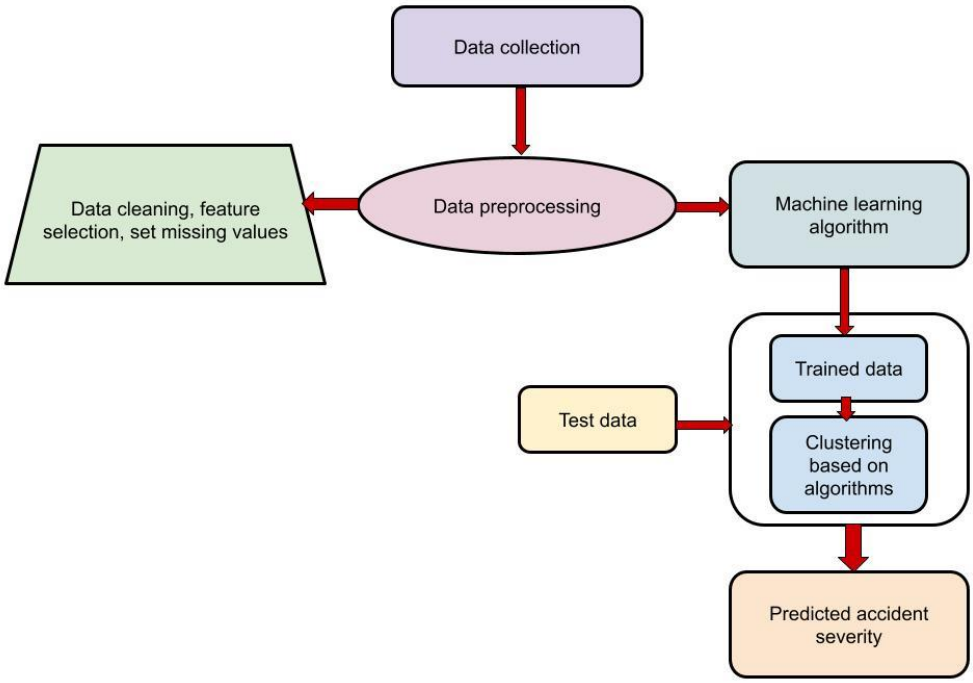

Figure-1 flowchart for proposed model

Since each variable reflects a unique set of qualities, there are no conflicts between the attributes when the input and output variables are taken into account. Numbers have already been used to classify and represent variables. There are seven categories for the type of accident that happened: angle, rear-end, head-on, rear-to-rear, sideswipe in the same direction, and sideswipe in the other way. Dataset was limited to head-on collisions only since they have the highest percentage of fatal injuries. There are 10,386 records of head-on collisions, 160 of which indicate a fatal injury; the first point of impact in all 160 of these events is classified as front. There are nine categories at the initial point of impact: front, right side, left side, back, front right corner, front left corner, back right corner, and back left corner. There is also no damage or non-collision. 10,251 recordings exist for head-on collisions with front impact, accounting for 98.70% of all head-on collision records (10,386 total). Due to this, we have eliminated the remaining 135 records and opted to concentrate just on front impact. Because there are an excessive number of entries in the dataset with unknown values, travel speed and speed restriction were not included in the model. In particular, the travel speed at the time of the accident and the local speed limit were unknown for 67.68% of the data.

4. Histogram residual Hopfield convolutional neural networks (HRHCNN) based segmentation:

Picture of intensity R, G, and B are the three colour channels used to compute I. I is equal to a gray-level image, hence the 1-D intensity histogram, or PDF, of that image can be calculated as eqn (1)

$$h_I(i) = \frac{1}{MN}\sum_{m=0}^{M-1}\sum_{n=0}^{N-1}\delta(I(m,n)-i),\ i = 0,\dots,L-1, \tag{1}$$

where L is the number of levels in the intensity image and M and N are the number of rows and columns in the image in eqn (2)

$$\delta(j) = \begin{cases} 1 & \text{if } j = 0 \\ 0 & \text{otherwise} \end{cases} \tag{2}$$

Next, the global HE function FI is ascertained using the histogram in eqn (3)

$$F_I(i) = \left\lceil (L-1) \times \sum_{j=0}^{i} h_I(j) \right\rceil,\ i = 0, \ldots, L-1 \quad (3)$$

FI (I(m, n)) holds the new value provided by the global HE technique for each value I(m, n). The following represents the residual block with identity mapping and its formula (4)

$$x_{l+1} = x_l + F(x_l, W_l) \quad (4)$$

Residual blocks are layered one after the other to form residual network. These model configurations typically have three-by-three filters in their convolutional layers. Another key idea in architectural design is pooling layers, which reduce the spatial dimension of an image and provide significant computational power advantages. Utilizing max pooling layers of size 3 × 3 and a stride of 2 (3 × 3/ST.2), we perform a subsampling. All neurons are used during the test, but the likelihood is multiplied on their outputs. Probability of 0.5 is typically most utilized. This layer's drawback is that it almost doubles number of iterations required for convergence. For nearly all configurations, utilizing this layer with a probability of 0.5 lowers error rate to about 2%. Dropout layers are added following pooling layers and in between residual layers.

A Hopfield network is made up of a collection of linked neurons N that independently and asynchronously change their activation levels. The characteristic state of a neuron I is Si = ±1. The fundamental idea behind HNNs is to store binary patterns in the format {+1, −1} N, and then utilise Hebb's rule to learn them. These patterns are then predicted using a noisy input vector during the inference stage. Its noise resistance is highly intriguing for a variety of applications. The Hopfield networks' "energy" is determined by eqn (5)

$$E = -\frac{1}{2}\sum_{i,j}^{N} S_i S_j w_{ij} \quad (5)$$

With repeated updates, HNN will converge to a local minimum in energy function. Thus, the weights with the lowest energy function values are the ideal ones. Additionally, assuming the stability of every pattern, theoretical storage capacity of HNN is defined by eqn (6)

$$P_{\max} = \frac{N}{4\ln N} \quad (6)$$

Every pattern that is saved matches a local minimum of energy that is specified in eqn(6). New learning rules as well as energy functions that enhanced the features of Hopfield networks are proposed in a number of recent research. The amount of storage was approximately 0.138 × N. When Hebb's rule had no bearing on the learning rate, N patterns might be stored as stated in [40]. By utilising novel energy functions, like interaction functions with the formula F(x) = x n, a storage capacity proportional to Nn−1 could be achieved. During the inference stage, the input image's feature maps are extracted using the same pretrained CNN. The network that has resulted in the least amount of changes to the input pattern is then chosen. The goal of this well-known combinatorial optimisation problem is to identify the ideal object from a set of things. The standard 0–1 knapsack problem is described as N items, where the collection of items is denoted by N = {1, 2, 3,..., n} by eqn (7)

$$\begin{cases} \text{Maximize } \sum_{i=1}^{n} x_i p_i \\ \text{subject to, } \sum_{i=1}^{n} x_i w_i \le W \\ x_i \in \{0,1\} \end{cases} \quad (7)$$

Hopfield network can then be thought of as a knapsack that can contain a collection of objects, in this example, patterns that need to be stored. Every pattern has a weight wi, which is equal to absolute energy of pattern (x μ), as determined by eqn(8), and a value pi, which may be determined by calculating how similar the pattern is to the others. The following formula determines the knapsack W's capacity (or total weight):

$$W = \max\{|E_1|, |E_2|, \ldots, |E_n|\} \times P_{\max} \quad (8)$$

The upper bound of the HNN's theoretical capacity, as determined by (2), can be used to estimate Pmax. Using one of the popular similarity measures, the values of n separate objects (patterns) can be defined.

5. Markov belief gradient discriminant analysis (MBGDA):

HMM with I states and continual emissions. Let y = {y0, y1,..., yT } represent observed data series, with each yt ∈ R L. The l-th component of yt, which represents observation for l-th feature at time t, is shown by ylt. x = {x0,

x1,..., xT} represents succession of unseen states. A is transition matrix of Markov chain connected to this sequence. aij = P(xt = j|xt−1 = i) represents elements of this transition matrix, π represents the distribution of the starting state. With respect to these values, the full data likelihood is given as follows by eqn (9)

$$p(\mathbf{x}, \mathbf{y} \mid \Lambda) = \pi_{x_0} f_{x_0}(y_0) \prod_{t=1}^{T} a_{x_{t-1}, x x_0} f_{x_2}(y_t) \tag{9}$$

where fxt (yt) is emission distribution given state xt and 3 is set of model parameters. We employ a feature saliency method for emission distributions in order to pick features [11]. If a feature's distribution is influenced by the underlying state, it is deemed relevant; if it is not, it is deemed irrelevant. Let z = {z1,...,zL} be a set of binary variables that represent significance of every feature. The l-th characteristic is important if zl = 1. In every other case, the l-th characteristic is meaningless if zl = 0. Chance that the l-th feature is important is known as the feature saliency (ρl). Given z and x, the conditional distribution of yt can be expressed as follows, considering features are conditionally independent given state by eqn (10)

$$p(y_t \mid \mathbf{z}, x_t = i, \Lambda) = \prod_{l=1}^{L} r(y_{lt} \mid \mu_{il}, \sigma_{il}^2)^z q(y_{lt} \mid \epsilon_l, \tau_l^2)^{1-z}$$

$$P(\mathbf{z} \mid \Lambda) = \prod_{l=1}^{L} \rho_l^3 (1-\rho_l)^{1-z} \tag{10}$$

Given x, joint distribution of yt and z is given by eqn (11)

$$p(y_I, \mathbf{z} \mid x_I = i, \Lambda) = \prod_{l=1}^{L} [\rho_l r(y_{ll} \mid \mu_{ll}, \sigma_{il}^2)]^{3\pi} [(1-\rho_l) q(y_{ll} \mid \epsilon_l, \tau_l^2)]^{1-2} \tag{11}$$

After summing eqn(12) across z, marginal distribution for yt given x is as follows:

$$f_{x_t}(y_t) = p(y_t \mid x_t = i, \Lambda) = \prod_{l=1}^{L} \left(\rho_l r(y_{lt} \mid \mu_{il}, \sigma_{il}^2) + (1-\rho_l) q(y_{ll} \mid \epsilon_l, \tau_l^2) \right) \tag{12}$$

The gradient map is calculated given a labelled picture xi, and a collection of integral images of gradient magnitude at every orientation {{xi,1, {xi,2, · · ·, {xi,b} is obtained. Since the cell location (x0, y0, x1, y1) can fully represent all 9 corners of the 2 × 2 cells, each bin of the histogram may be evaluated by accessing integral image ¯xi,j at relevant pixel location, which is defined as follows by eqn (12)

$$h_{i,j} = \bar{\mathbf{x}}_{i,j}(x_0, y_0) + \bar{\mathbf{x}}_{i,j}(x_1, y_1) - \bar{\mathbf{x}}_{i,j}(x_0, y_1) - \bar{\mathbf{x}}_{i,j}(x_1, y_0), \tag{12}$$

and j ∈ [1, b], where i ∈ [1, K]. the greedy layer-wise unsupervised training procedure of a DBN with three hidden layers (h1, h2, and h3) from left to right and one input layer (x). Darker colour layers are still being trained, while lighter colour layers indicate previously trained layers. h3(x) represents x after the greedy layer-wise unsupervised learning. Subsequently, an output layer is placed at the top, and utilising labelled reviews, the weights are adjusted for better discriminative capability. Its foundation is the notion that a sample belongs to a class if most of k most similar samples of that sample in a given feature space also belong to that class. The proposed fitness function considers the accuracy of feature classification. The accuracy of classification is higher when there is a correlation among the features in the subset. Less features in the subset lead to higher classification accuracy. One of the objectives of FS technique is to have a higher classification accuracy; recalculating number of choosed features is another key goal; the fewer features in the solution, the better. The fitness function's mathematical formulation is displayed below eqn (13)

$$\text{fitmess} = \alpha \gamma_R(D) + \beta \frac{|M|}{|N|} \tag{13}$$

In this case, the time complexity and space complexity are influenced by each other. Performance of the space complexity may suffer when a better time complexity is pursued, which could result in the need for more storage space; conversely, the time complexity may suffer when a better space complexity is pursued, which could result in a longer running time. We must find a balance between the incompatibilities of time and space complexity. belief distribution structure, rule weight parameter, rule antecedent attribute parameter to the expression form of belief rules by eqn (14)

$$R_k\text{: if } \{X_1 \text{ isA } A_1^k \wedge \cdots \wedge X_{T_i} isA_{T_k}^k\} \text{ then } \{(D_1, \beta_1^k), \cdots, (D_N, \beta_N^k)\}, \sum_{i=1}^{N} \beta_i^k \leq 1 \tag{14}$$

When the rule information is finished, the equal sign is produced. Each antecedent attribute has a weight of δ1, δ2, · · ·, δTk, and each rule has a weight of θk. Reference value chosen by rule for ith attribute is represented by

A k i, rule's degree of conviction in the ith consequent attribute is shown by β k i. Because of this, extended belief rule base system gives antecedent attributes a belief distribution structure. Rule form of this system is as follows by eqn (15)

$$R_k: \text{if } \left\{\left[\left(A_{11}^k, \alpha_{11}^k\right), \cdots, \left(A_{1J_1}^k, \alpha_{1J_1}^k\right)\right] \wedge \cdots \wedge \left[\left(A_{T_2}^k, \alpha_{T_2 1}^k\right), \cdots, \left(A_{T_k J_{T_2}}^k, \alpha_{T_k J_{T_k}}^k\right)\right]\right.$$

$$\alpha_{ij}^k = \frac{\gamma_{i(j+1)} - x_i^k}{\gamma_{i(j+1)-}^k}, \gamma_{ij} \leq x_i^k \leq \gamma_{i(j+1)} \quad (15)$$

Values of the original data on other qualities can be transformed into corresponding belief distribution form using same conversion process. Using this method, belief distribution form of rule consequent attribute can also be obtained.

6. Simulation analysis:

Data Exploration

Python comes with a drawing library called Matplotlib. This visualisation technique is used to analyse and tally the frequency and severity of the accidents. This method investigates possible connections between the severity of an accident and a number of variables, including the weather, lighting, road surface. Results can assist road managers in identifying as well as avoiding potential risk factors in order to lower the probability of serious accidents. There are three categories for the accident's severity. Traffic incidents classified as Level 1 are the most severe, resulting in a high number of victims. Level 3 collisions are the most frequent and mild, resulting in fewer car crashes and casualties. As a result, the percentage of accidents at each of the three severity levels under diverse conditions may be seen in the pie chart.

Dataset: The data used in this study came from Australian Road Deaths Database (ARDD). This database includes statistics on Australian road transport fatalities that police agencies submit to state and local road safety organisations on a monthly basis. ARDD gathers collision data and demographic data for Australians who lost their lives in auto accidents. A road death, also referred to as a fatality, happens when someone passes away within 30 days following an automobile collision as a result of their injuries. Any incident in which a pedestrian is killed is considered a pedestrian crash in this dataset, regardless of number of autos involved. Thirteen of twenty-four columns and variables in the ARDD can be used to predict pedestrian crashes. It is important to note that the study used most recent available data, which were gathered between 1989 and 2021. The whole dataset, with a sample size of 52,843, was utilised to predict pedestrian fatalities. An overview of factors employed in this study is given in Table 2. This dataset contains fundamental data regarding the PDRC. By adjusting for these characteristics, we were able to accomplish the study's goal of using pedestrian crash data to apply the combination of neural networks and Bayesian theory. By utilising datasets including other factors in the future, this study can be expanded.

The data used in this investigation were taken from the National Automotive Sampling System (NASS) General Estimates System (GES). Goal of the GES datasets is to provide nationally representative probability sampling from estimated 6.4 million accident reports that are reported in US each year. 417,670 traffic accident reports spanning the years 1995 to 2000 made up the study's initial dataset. According to variable definitions of GES dataset, passenger information is not included; the only records in this dataset are those of the drivers. Severity of an injury can be divided into five categories: likely, incapacitating, non-incapacitating, fatal, and no damage. In the original dataset, the percentage of instances with no harm (70.18%), potential injury (16.07%), non-incapitating injury (9.48%), incapacitating injury (4.02%), and fatal injury (0.25%) were all reported.

The Central Bureau of Statistics (ICBS) of Israel provided the input data, which included 47,432 pedestrian-related traffic crashes between 2009 and 2019. Of these, 46,040 crashes resulted in non-fatal injuries to pedestrians, while 1392 crashes were fatal. 56 factors were included in the dataset: the crash's unique ID; year, date, time of collision; characteristics of the driver and pedestrian (such as age group); the crash's location; and road features. Every one of the fourteen CSV files used by the Israeli control authorities to keep track of road accidents in Israel has a unique structure. Using SQL Server's data transformation utilities, the collection of files was imported into a relational database in order to guarantee the integrity of incoming data and to expedite, improve, and enhance the data querying process. Three main entities are established within this framework: the

vehicle, the injured person, and the accident. Columns labelled "Accident ID" were provided for both the Vehicle and Injured Person records, matching those in the Accident table. Data synchronisation between the tables was made possible by this integrated design. Strict data integration procedures were implemented to guarantee data integrity. These included setting up foreign and unique indexes, default values, and the proper column data types (such as dates, floats, and integers). The Vehicle and Injured Person tables were additionally subjected to foreign key indexes.

7. Parameter metrics:

In order to prevent biases and overfitting during model training, this work arbitrarily divided a single dataset into five different subdivisions with roughly equal quantities of data points using k-fold cross-validation technique. Using following set of criteria, the effectiveness of the suggested methods in categorising as well as predicting pedestrian fatalities from traffic crashes was evaluated:

• Average training accuracy (ATA): Total number of accurate forecasts over two classes divided by total number of forecasts is the definition of prediction accuracy in binary class case of this study.

• Average F-1 score: To estimate criteria for each classification in binary-class forecasting study, average MCC was used. Average was computed by calculating number of accurately anticipated occurrences.

• Area under receiver operating characteristic curve (AUC): In this study, AUC was used to evaluate a scoring classifier at several cutoff points. Method capacity to discriminate between positive as well as negative categories is gauged by its AUC.

• Matthew's correlation coefficient (MCC): In this study, MCC was utilised to evaluate accuracy of binary classifications. Since MCC takes into account both true and erroneous positives and negatives, it is a balanced measure that may be utilized even in cases when categories have sizes that are noticeably different from one another. This standard is a correlation coefficient, which yields a value for the actual and predicted binary classes between -1 and +1.

8. Comparative analysis:

Table-1 Comparative analysis between proposed and existing technique for ARDD dataset

Technique	ATA	AUC	Average F-1 score	Recall	MCC
BNN	77	73	70	78	75
RF-LR	83	80	78	84	79
HRHCNN_MBGDA	90	85	91	94	83

Firstly, instead of only assigning a clear class label, it offers predictions for each class in the form of probabilities. This makes it possible to comprehend the model's predictions on a more complex level. Second, by giving the standard deviation of the posterior prediction, it also offers an approximation of degree of prediction uncertainty. This shows range of prediction and the degree of confidence that can be placed in it.

Table-2 Comparative for NASS dataset

Technique	ATA	AUC	Average F-1 score	Recall	MCC
BNN	74	77	80	75	69
RF-LR	82	80	85	83	74
HRHCNN_MBGDA	93	87	95	92	95

Table-3 Comparative for ICBS dataset

Technique	ATA	AUC	Average F-	Recall	MCC

			1 score		
BNN	80	72	69	75	76
RF-LR	84	78	73	80	83
HRHCNN_MBGDA	98	85	82	90	96

The above table-1-3 shows Comparative based on various smart grid security dataset. The dataset analysed are MIMIC-IV, NASS , ICBS dataset in terms of ATA, AUC, Average F-1 score, recall, MCC. When every prediction result is the level that appears the most frequently in the training dataset, accuracy of test dataset is equal to accuracy of baseline method. There's no need to accept and use the freshly built model if its accuracy is less than that of the benchmark. On the other hand, it is demonstrated that the newly constructed model, which has the better precision, is required for this investigation if its accuracy is noticeably higher than that of the baseline model.

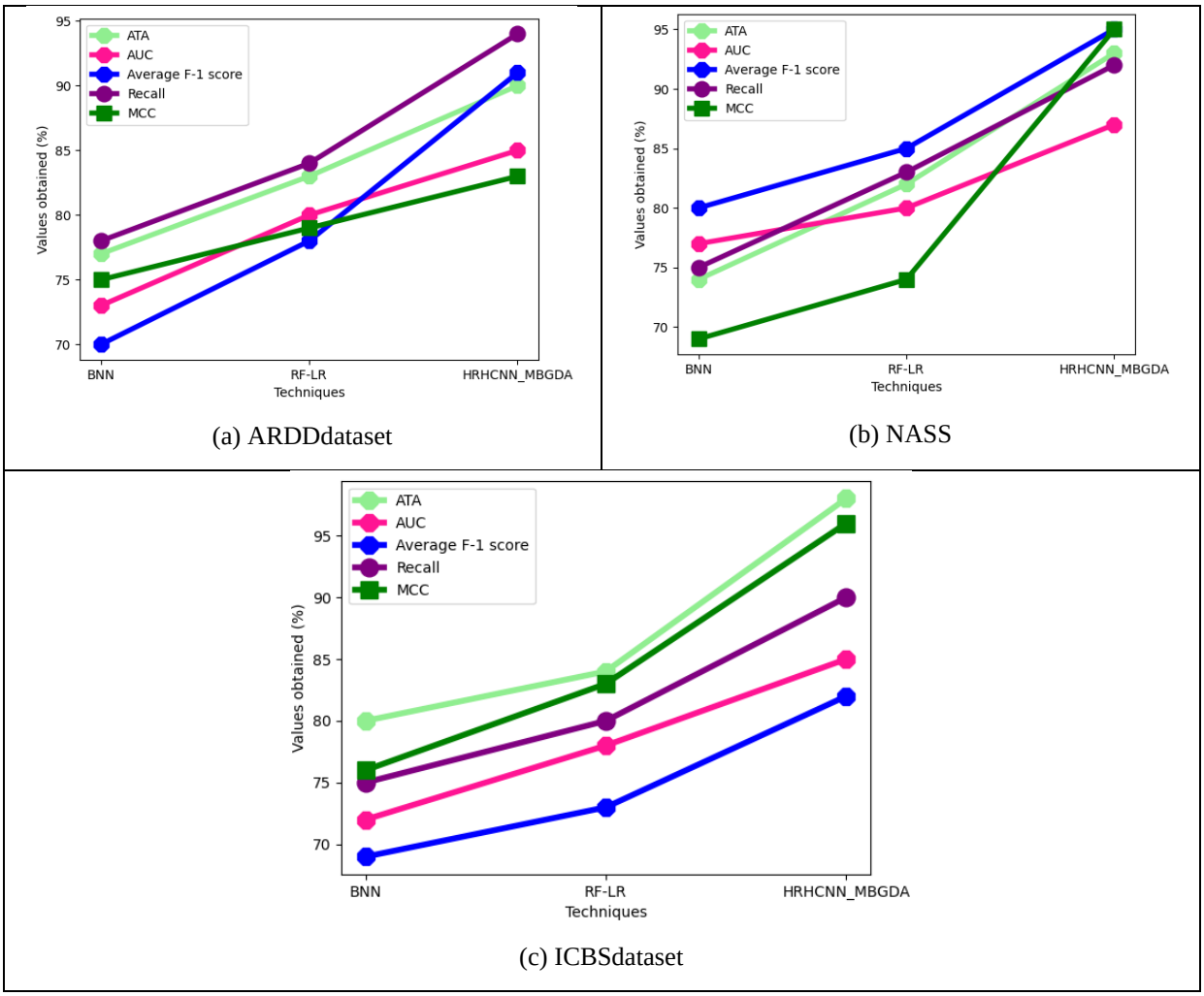

(a) ARDDdataset

(b) NASS

(c) ICBSdataset

Figure-2 (a)- (c) parametric analysis of existing BNN for (a) MIMIC-IV, (b) NASS **, (c)** ICBSdataset

The above figure 2 (a)- (c) shows parametric analysis of existing BNN in ARDDdataset. For ARDD dataset the existing BNN attained Average F-1 score of 70%, recall of 78%, AUC of 73%, ATA of 77%, MCC of 75%. Average F-1 score of 74%, recall of 75%, AUC of 77%, ATA of 74%, MCC of 69% for NASS ; existing BNN attained Average F-1 score of 69%, recall of 75%, AUC of 72%, ATA of 80%, MCC of 76% for ICBSdataset. Data and issues are necessary for building an appropriate neural network architecture. In order to create non-linearity in the neuron's output, the authors first employed a rectified linear unit (ReLU) as the activation function between the succeeding hidden layers. A batch size of 64 samples from training dataset was used to compute the error gradient. Different learning rates (LRs) for Adam optimizer operation (10-3, 10-2, 10-1) were assessed in order to identify error gradient of method optimisation during learning stage.

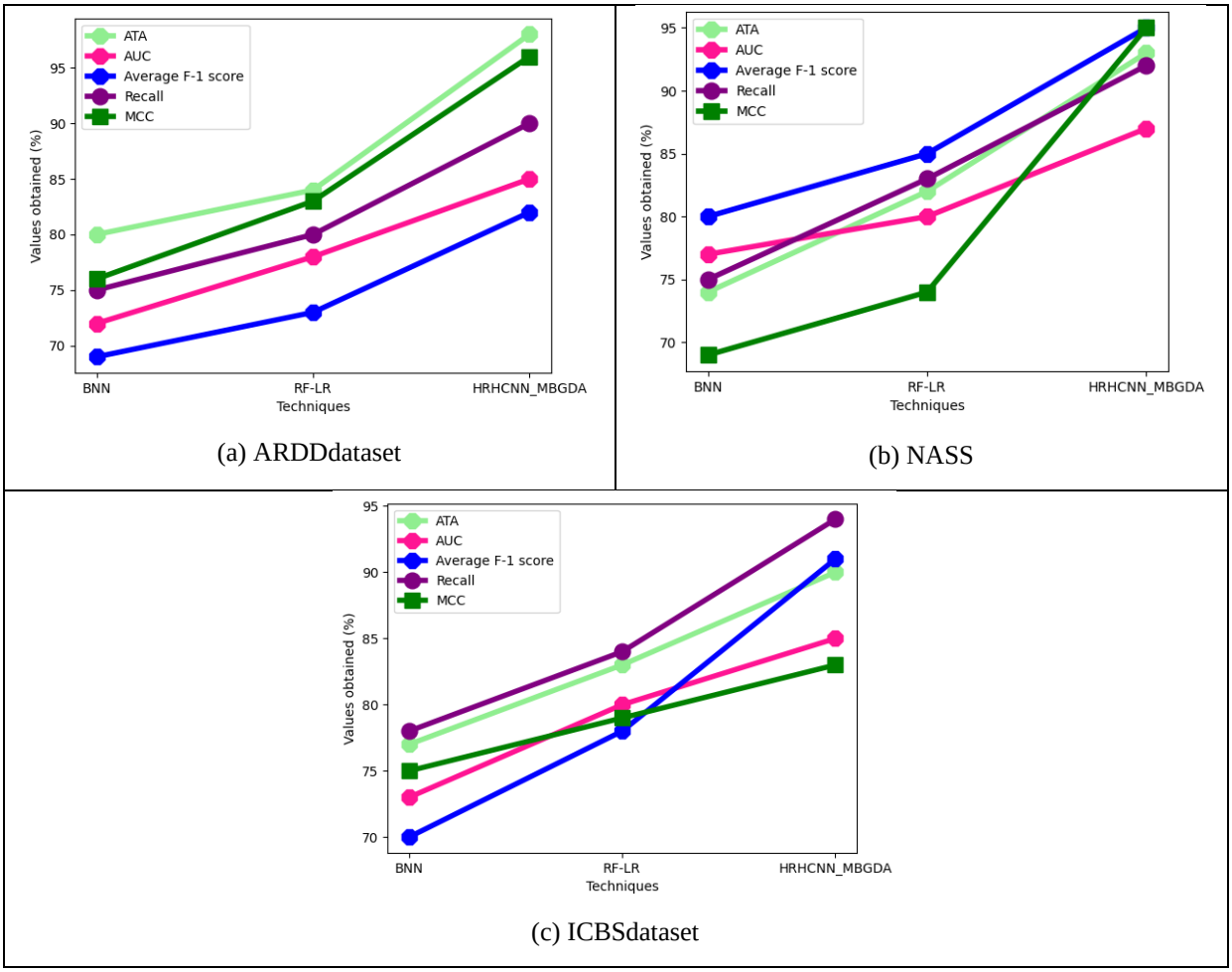

(a) ARDDdataset

(b) NASS

(c) ICBSdataset

Figure-3 (a)- (c) parametric analysis of existing RF-LR for (a) MIMIC-IV, (b) NASS , (c) ICBSdataset

Figure 3(a)–(c) above displays a parametric analysis of the RF-LR that is currently in use in the ARDDdataset. The current RF-LR achieved Average F-1 score of 78%, recall of 84%, AUC of 80%, ATA of 83%, and MCC of 79% on the ARDDdataset. For the NASS , the existing RF-LR achieved Average F-1 score of 85%, recall of 83%, AUC of 80%, ATA of 82%, and MCC of 74%; Average F-1 score of 73%, recall of 80%, AUC of 78%, ATA of 84%, MCC of 83% for ICBSdataset.

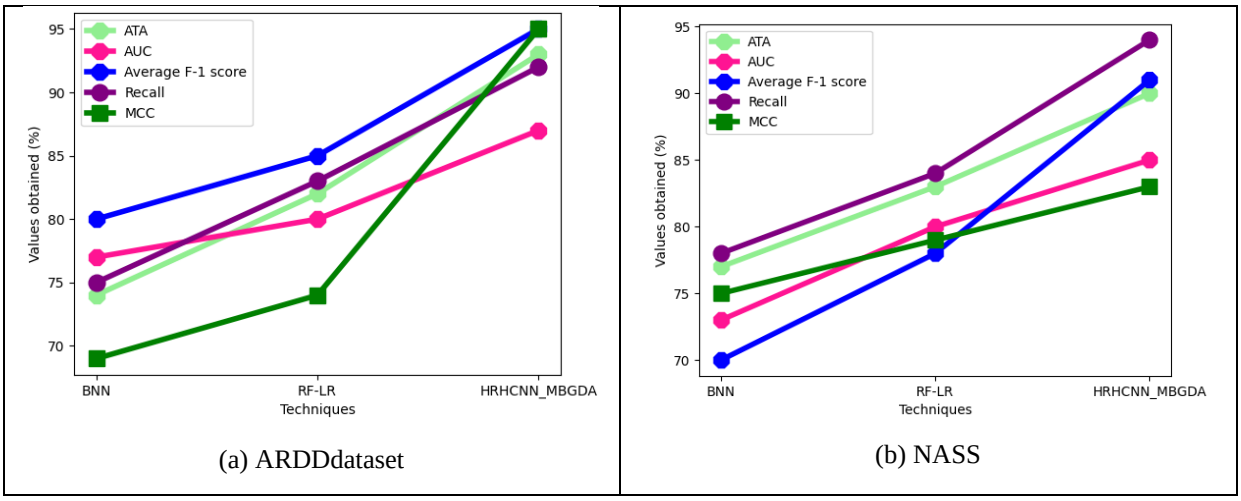

(a) ARDDdataset

(b) NASS

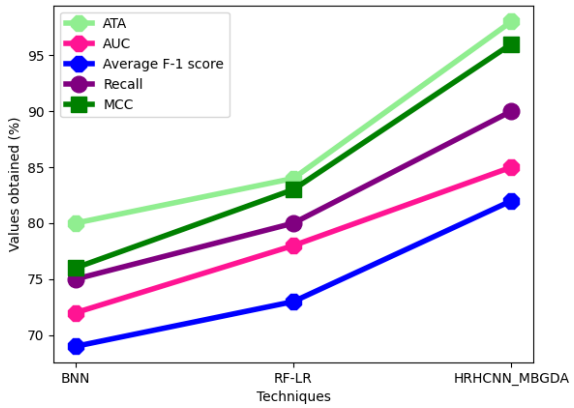

(c) ICBSdataset

Figure-4 (a)- (c) parametric analysis of GBDNN_SCQ-SwMO for (a) MIMIC-IV, (b) NASS , (c) ICBSdataset

The parametric analysis of HRHCNN_MBGDA in the ARDDdataset is displayed in the above figure 4(a)–(c). HRHCNN_MBGDA achieved 91% Average F-1 score, 94% recall, 85% AUC, 90% ATA, and 83% MCC for the ARDDdataset. For the NASS , Average F-1 score was 93%, recall was 92%, AUC was 87%, ATA was 93%, and MCC was 95%. For the ICBSdataset, Average F-1 score was 82%, recall was 90%, AUC was 85%, ATA was 98%, and MCC was 96%. Most records had same accident severity and number of casualties, per dataset's statistical analysis conclusion. More than 90% of automobile accident reports have many casualties of 1, and more than 95% have severity level 3, which is the lowest severity. Stated differently, the majority of dataset's records pertain to minor accidents. The sensitivity of the model is decreased during the modelling step when numerous records with disparate attributes are assigned to the same label. The high accuracy is not unexpected, as the model does a good job of predicting little incidents. This is due to the fact that splitting a dataset into training and testing increases the likelihood that numerous little occurrences will be included in the testing data. On the other hand, the number of vehicles engaged in the collision has a wider range of possible values, indicating that more pertinent factors could influence the outcome. As a result, the classification model's accuracy is inferior to that of the other two labels.

9. Conclusion:

Based on pedestrian recognition in picture analysis, a novel deep learning model has been suggested in this research for the investigation of highway traffic accidents. In this case, histogram residual Hopfield convolutional neural networks (HRHCNN) were used to gather and analyse the highway traffic photos for pedestrian recognition, and markov belief gradient discriminant analysis (MBGDA) was used to pick features. The segmentation selected features display the pedestrian involved in a highway traffic collision. According to our trials, the non-incapacitating, incapacitating, and lethal injury classes all had classification accuracy that was above 95%. Neural networks underperformed the hybrid technique for both the no injury and potential injury groups. Decision trees would be the most effective method for directly modelling the no injury and potential injury classes. The primary goal of previous study was to differentiate between the injury (including fatality) and no-injury classes. We expanded the study to include courses for potential injuries, incapacitating injuries, nonincapacitating injuries, and fatal injuries. The model for both fatal and non-fatal injuries outperformed the other classifications, according to our trials. Predicting both fatal and non-fatal injuries is crucial because the largest financial and social burden on society is borne by drivers' fatalities. Generally speaking, the findings don't show a clear major reversal of the cause. However, a relative safer zone and a dangerous zone can be identified. Most often, speeding, careless driving, and forceful driving result in fatal injuries. But in comparison to other areas, roads with little or no illumination play a large role in creating problems.

Funding :

This work was sponsored in part by2023 University Scientific Research Platform and Scientific Research Project Characteristic Innovation Project of Guangdong Provincial Department of Education: " Research on the

optimization scheme of passenger transfer connection in Guangzhou South Railway Station ". Subject No. 2023WTSCX243

Reference:

[1] Devipriya, A., Prabakar, D., Singh, L., Oliver, A. S., Qamar, S., & Azeem, A. (2023). Machine learning-driven pedestrian detection and classification for electric vehicles: integrating Bayesian component network analysis and reinforcement region-based convolutional neural networks. *Signal, Image and Video Processing*, *17*(8), 4475-4483.

[2] Balasubramanian, S. B., Balaji, P., Munshi, A., Almukadi, W., Prabhu, T. N., Venkatachalam, K., & Abouhawwash, M. (2023). Machine learning based IoT system for secure traffic management and accident detection in smart cities. *PeerJ Computer Science*, *9*, e1259.

[3] Hossain, A., Sun, X., Shahrier, M., Islam, S., & Alam, S. (2023). Exploring nighttime pedestrian crash patterns at intersection and segments: Findings from the machine learning algorithm. *Journal of safety research*, *87*, 382-394.

[4] Hussain, F., Ali, Y., Li, Y., & Haque, M. M. (2024). Revisiting the hybrid approach of anomaly detection and extreme value theory for estimating pedestrian crashes using traffic conflicts obtained from artificial intelligence-based video analytics. *Accident Analysis & Prevention*, *199*, 107517.

[5] Loo, B. P., Fan, Z., Lian, T., & Zhang, F. (2023). Using computer vision and machine learning to identify bus safety risk factors. *Accident Analysis & Prevention*, *185*, 107017.

[6] Azhar, A., Rubab, S., Khan, M. M., Bangash, Y. A., Alshehri, M. D., Illahi, F., & Bashir, A. K. (2023). Detection and prediction of traffic accidents using deep learning techniques. *Cluster Computing*, *26*(1), 477-493.

[7] Sattar, K., Chikh Oughali, F., Assi, K., Ratrout, N., Jamal, A., & Masiur Rahman, S. (2023). Transparent deep machine learning framework for predicting traffic crash severity. *Neural Computing and Applications*, *35*(2), 1535-1547.

[8] Sumi, A., & Santha, T. (2023, May). Analysis of Machine Learning Approaches to Detect Pedestrian Under Different Scale Using Frame Level Difference Feature. In *International Conference on Computational Sciences and Sustainable Technologies* (pp. 464-473). Cham: Springer Nature Switzerland.

[9] Khan, M. N., Das, S., & Liu, J. (2024). Predicting pedestrian-involved crash severity using inception-v3 deep learning model. *Accident Analysis & Prevention*, *197*, 107457.

[10] Al Sulaie, S. (2023, February). Golden jackal optimization with deep learning-based anomaly detection in pedestrian walkways for road traffic safety. In *International conference on innovative computing and communication* (pp. 617-636). Singapore: Springer Nature Singapore.

[11] Jun, H. J., Jung, S., Kang, S., Kim, T., Cho, C. H., Jhoo, W. Y., & Heo, J. P. (2024). Factors associated with pedestrian-vehicle collision hotspots involving seniors and children: a deep learning analysis of street-level images. *International Journal of Urban Sciences*, *28*(2), 359-377.

[12] Ahmed, S., Hossain, M. A., Ray, S. K., Bhuiyan, M. M. I., & Sabuj, S. R. (2023). A study on road accident prediction and contributing factors using explainable machine learning models: analysis and performance. *Transportation research interdisciplinary perspectives*, *19*, 100814.

[13] Lian, T., Loo, B. P., & Fan, Z. (2024). Advances in estimating pedestrian measures through artificial intelligence: From data sources, computer vision, video analytics to the prediction of crash frequency. *Computers, environment and urban systems*, *107*, 102057.

[14] Pérez-Sala, L., Curado, M., Tortosa, L., & Vicent, J. F. (2023). Deep learning model of convolutional neural networks powered by a genetic algorithm for prevention of traffic accidents severity. *Chaos, Solitons & Fractals*, *169*, 113245.

[15] Melegrito, M., Reyes, R., Tejada, R., Anthony, J. E. S., Alon, A. S., Delmo, R. P., ... & Anqui, A. P. (2024, April). Deep Learning Based Traffic Accident Detection in Smart Transportation: A Machine Vision-Based Approach. In *2024 4th International Conference on Applied Artificial Intelligence (ICAPAI)* (pp. 1-6). IEEE.

[16] Adewopo, V. A., & Elsayed, N. (2024). Smart city transportation: Deep learning ensemble approach for traffic accident detection. *IEEE Access*.